Received: 28 April 2022 | Revised: 2 June 2022 | Accepted: 3 June 2022

DOI: 10.1002/sus2.76

RESEARCH ARTICLE

SusMat WILEY

Surface decorated Ni sites for superior photocatalytic hydrogen production

Wenhuan Huang[1,2] | **Tingting Bo**[3] | **Shouwei Zuo**[2] | **Yunzhi Wang**[2] | **Jiamin Chen**[1] | **Samy Ould-Chikh**[2] | **Yang Li**[2] | **Wei Zhou**[3] | **Jing Zhang**[4] | **Huabin Zhang**[2]

[1]Key Laboratory of Chemical Additives for China National Light Industry, College of Chemistry and Chemical Engineering, Shaanxi University of Science and Technology, Xi'an, China

[2]KAUST Catalysis Center (KCC), King Abdullah University of Science and Technology (KAUST), Thuwal, Saudi Arabia

[3]Department of Applied Physics, Tianjin Key Laboratory of Low Dimensional Materials Physics and Preparing Technology, Faculty of Science, Tianjin University, Tianjin, China

[4]Beijing Synchrotron Radiation Facility, Institute of High Energy Physics, Chinese Academy of Sciences, Beijing, China

Correspondence
Huabin Zhang and Samy Ould-Chikh, KAUST Catalysis Center (KCC), King Abdullah University of Science and Technology (KAUST), Thuwal 23955-6900, Saudi Arabia.
Email: Huabin.zhang@kaust.edu.sa; samy.ouldchikh@kaust.edu.sa

Wei Zhou, Department of Applied Physics, Tianjin Key Laboratory of Low Dimensional Materials Physics and Preparing Technology, Faculty of Science, Tianjin University, Tianjin 300072, China.
Email: weizhou@tju.edu.cn

Funding information
King Abdullah University of Science and Technology; National Natural Science Foundation of China, Grant/Award Number: 22001156; Youth Talent Promotion Project of the Science and Technology Association of the Universities of Shaanxi Province, Grant/Award Number: 20210602

Abstract

Precise construction of isolated reactive centers on semiconductors with well-controlled configurations affords a great opportunity to investigate the reaction mechanisms in the photocatalytic process and realize the targeted conversion of solar energy to steer the charge kinetics for hydrogen evolution. In the current research, we decorated isolated Ni atoms on the surface of CdS nanowires for efficient photocatalytic hydrogen production. X-ray absorption fine structure investigations clearly demonstrate the atomical dispersion of Ni sites on the surface of CdS nanowires. Experimental investigations reveal that the isolated Ni atoms not only perform well as the real reactive centers but also greatly accelerate the electron transfer via direct Ni–S coordination. Theoretical simulation further documents that the hydrogen adsorption process has also been enhanced over the semi-coordinated Ni centers through electronic coupling at the atomic scale.

KEYWORDS
electron transfer, hydrogen evolution, molecular activation, photocatalysis, single atom catalyst

1 | INTRODUCTION

The highly increased energy demand of modern society has attracted enormous attention for developing renewable and clean energy sources, among which solar energy is considered as a promising candidate.[1–7] Photo-driven water splitting has been regarded as a sustainable and cost-efficient strategy to generate clean hydrogen (H_2) fuel to realize a stable supply of renewable energy.[5,8,9] Semiconductor materials have received great research attention due to their unique chemical, physical, and optoelectronics characteristics. Nevertheless, the catalytic performance over those semiconductive materials is relatively low even under the participation of sacrificial agents. Recombination of photoexcited electron–hole pairs before the redox reaction is considered as the main reason for the low efficiency.[10–12] Cocatalysts are usually applied in photocatalytic systems to accelerate the separation of photogenerated electron/hole and *in-fine* improving the reaction kinetics. Numerous researches have confirmed that Pt affords the highest hydrogen evolution rates among various cocatalysts. However, the practical utilization of Pt-based cocatalysts is highly hindered by their high cost and scarcity. Therefore, developing cost-efficient and highly active alternatives to Pt is urgently expected.[13,14] The development of precious metal-free cocatalysts that can be readily used for low-cost and pilot system design is thus significantly favored but still challenging to date.

Generally speaking, charge separation through the capture of electrons by a cocatalyst affords the most powerful strategy to enhance the hydrogen evolution rates in the reaction solution.[15–18] Manipulating the size of the cocatalyst down to a single-atom state represents the highest utilization of metal species, which may also improve the photogenerated electron–hole separation efficiency.[19–23] Furthermore, homogeneously dispersed isolated reactive centers offer us an ideal model to explore the precise structure–performance correlation at the atomic level. The electronic structure of isolated reactive centers as cocatalysts and their interaction with light absorbers are important factors in the comprehension of the photocatalytic mechanism.[24–27] Single-atom catalysts, with nearly identical catalytically reactive centers, have emerged as excellent candidates for photocatalysts, affording us the great chance to detect their structural evolution during the catalytic process.[6] Moreover, the decoration of isolated active centers over semiconductors may also induce the generation of discrete energy bands, which is very effective in trapping charge carriers and boosting the transfer of photogenerated electrons and holes.[28–30] Considering these characteristics, it is reasonable to expect greatly boosted catalytic performance for photocatalytic water splitting over single atom-decorated semiconductor photocatalysts.

Herein, we successfully decorated isolated Ni atoms (the cocatalyst) onto the surface of CdS nanowires (denoted CdS@Ni) for efficient photocatalytic H_2 evolution. Synchrotron radiation-based X-ray absorption spectroscopy has been applied to determine the coordination configuration of the isolated reactive centers. Photocatalytic water splitting performance evaluation undoubtedly demonstrates that the decorated Ni atoms work as the active centers for proton recombination, steering the charge kinetics and improving the photocatalytic activities dramatically. Density functional theory (DFT) simulations further demonstrate that the energy band configuration of the CdS semiconductor has been obviously changed after Ni decoration, resulting in an obviously reduced work function and greatly reduced Gibbs free energy for the adsorption of H*.

2 | SYNTHESIS AND STRUCTURE CHARACTERIZATION

A solvothermal approach is applied for constructing CdS nanowires.[8] The successful synthesis of CdS with a hexagonal wurtzite crystal structure is verified by X-ray diffraction (XRD) measurements (Figure S1). Scanning transmission electron microscopy (STEM) investigations verify the one-dimensional nanowires in morphology with a uniform dispersion in diameter (Figure S2). Isolated Ni atoms are further loaded onto the surface of the CdS nanowire via a facile wet-chemical method, followed by heat treatment to enhance the interaction between the isolated Ni atoms and CdS supports via the newly generated Ni–S bonding (Figure 1A). It should be noted that the crystal structure of the hexagonal wurtzite crystal structure of CdS did not change after the decoration of Ni species, as evidenced by the well-maintained XRD pattern, no peak indexed to the crystallographic Ni is presented (Figure S3). As confirmed by transmission electron microscopy (TEM) observation, no noticeable morphology of CdS nanowires can be detected with the decoration of isolated Ni atoms over the surface (Figure 1B,C). High-resolution TEM images with various magnifications of the CdS@Ni sample clearly reveal the absence of Ni or NiO_x clusters (Figure 1D–F). The interplanar distance is confirmed as 3.4 Å, which can be ascribed to the (002) plane of hexagonal CdS, which is also consistent with the (002) spacing distance evaluated from the selected area electron diffraction spots (Figure 1G).[31,32] The unvaried lattice fringes of CdS further demonstrate that the original structure of CdS is not changed after Ni decoration.[33,34] All these results also suggest that the distribution of isolated

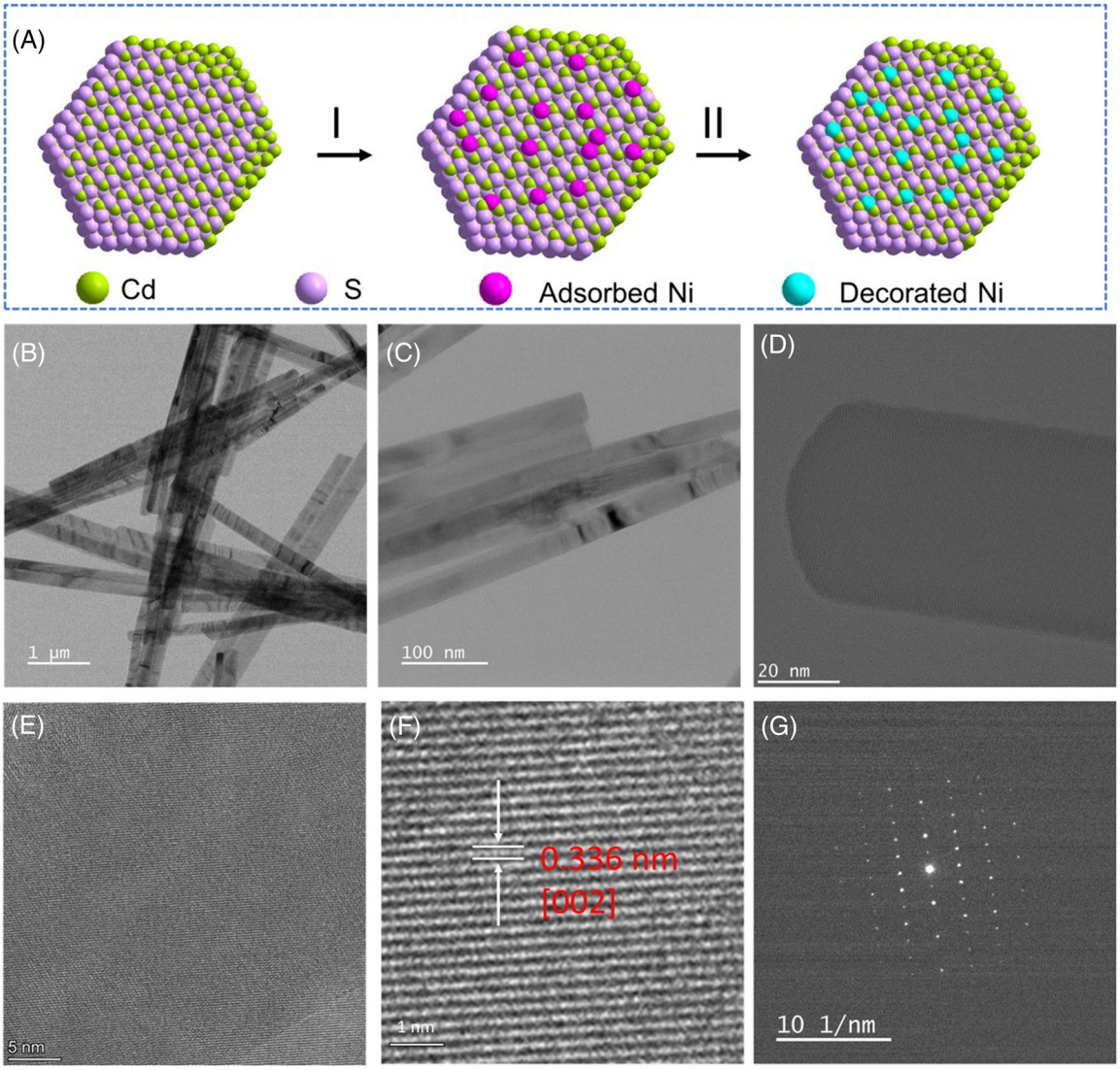

FIGURE 1 (A) Schematic illustration of the synthetic process of CdS@Ni: (I) surface adsorption of Ni species; (II) heat-treatment for enhancing the interaction between the isolated Ni atoms and CdS surface. (B and C) Transmission electron microscopy (TEM) images of CdS@Ni. (D–F) High-resolution TEM (HRTEM) image of CdS@Ni. (G) Selected area electron diffraction (SAED) pattern of CdS@Ni

Ni atoms is either grafted on the CdS surface or should follow the periodic arrangement of Cd atoms in CdS.[35,36] Catalysts with various Ni loading contents have also been synthesized. Inductively coupled plasma–optical emission spectrometry (ICP–OES) investigations confirm that the loading contents of Ni range from 0.29% to 1.68%. The Raman spectra have also been investigated for CdS- and Ni-decorated CdS@Ni, where the first-order LO Raman peak and second LO phonon vibrational peak appear at 297.9 and 598.1 cm^{-1}, respectively (Figure S4).[37] The observed LO Raman peak positions agree very well with those reported for CdS in the hexagonal wurtzite phase. The nearly identical vibration mode of these two samples also suggests that the Ni decoration cast limited influence on the surface of CdS. The Brunauer–Emmett–Teller surface areas of CdS and CdS@Ni were confirmed as 19.58 and 26.75 $m^2\ g^{-1}$, respectively, indicating the highly dispersed states of the nanowires (Figure S5).[38]

Extended X-ray absorption fine structure (EXAFS) spectrometry at the Ni K-edge has been explored using both wavelet transform (WT) and Fourier transformation to shed light on the local coordination geometry and oxidation state of the decorated Ni atoms. In the Fourier-transformed (FT)-EXAFS curve of CdS@Ni, a major peak around 1.86 Å assigned to the Ni–S coordination is clearly observed, while no Ni–Ni connection around 2.19 Å or Ni–O bond at 1.59 Å is detected, validating that Ni atoms are isolated and stabilized by the S atoms from the CdS without the formation of oxide and Ni aggregation (Figure 2A). The WT simulation has been conducted to afford radial distance resolution in the K space. The WT intensity maximum at about 6.1 $Å^{-1}$ arising from the Ni–S coordination

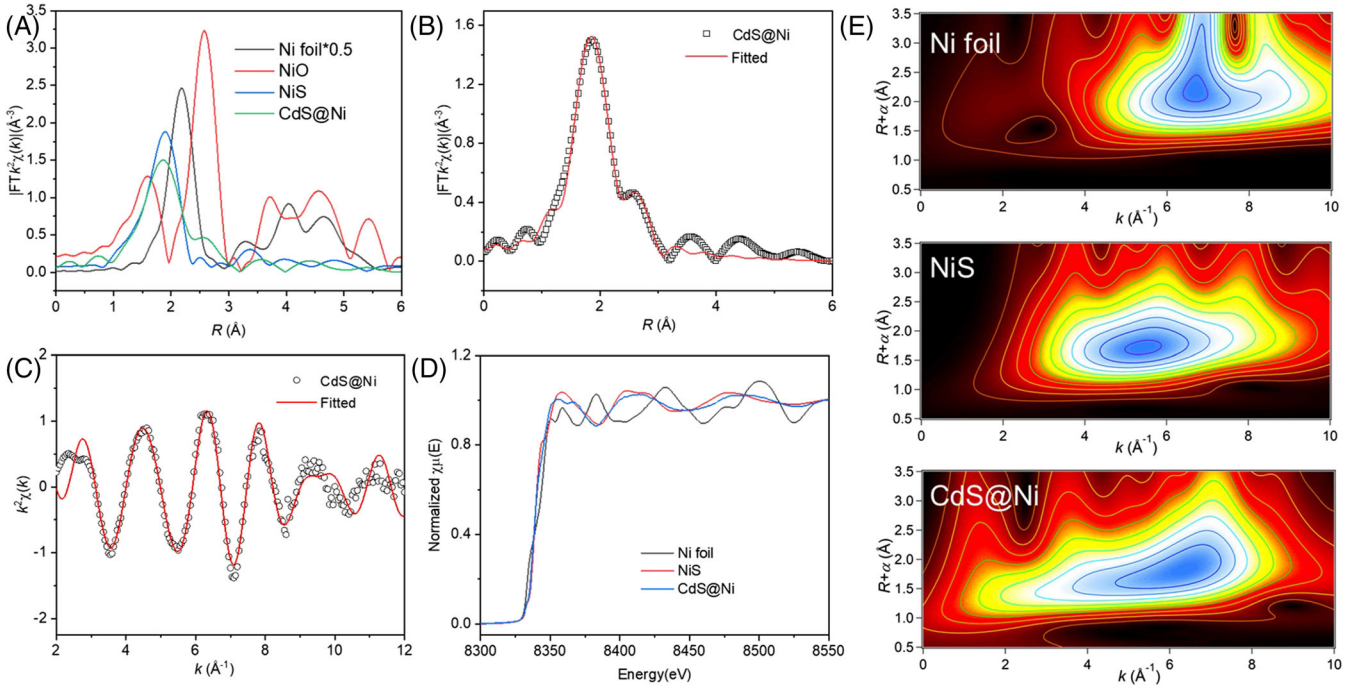

FIGURE 2 (A) Fourier transform magnitudes of the experimental Ni K-edge extended X-ray absorption fine structure (EXAFS) spectra in R space. (B and C) Fourier transform magnitudes of Co K-edge EXAFS spectra in R space (B) and K space (C). (D) Ni K-edge X-ray absorption near-edge structure (XANES) experimental spectra. (E) Wavelet transform (WT) for the k^3-weighted EXAFS signal

is well resolved at 1.0–3.0 Å for CdS@Ni, whereas an intensity maximum at about 6.64 $Å^{-1}$ associated with the Ni–Ni coordination is not detected (Figure 2E). These results further demonstrate that the Ni species in CdS@Ni should be isolated without any aggregation. The least-squares EXAFS curve-fitting analysis clarifies the coordination sphere of the atomically dispersed centers. The best-fitted results clearly confirm that the Ni–S bond length of 2.26 Å, much shorter than the Ni–Ni bonding (2.48 Å) in Ni foil (Figures 2B,C and S6). Further analysis demonstrates that the coordination number for the Ni–S bonding is about 4.3 in the first coordination sphere (Table S1).[39,40] As shown in Figure 2D, the X-ray absorption near-edge structure (XANES) curve of CdS@Ni at the Ni K-edge has displayed varied near-edge absorption energy from that of Ni foil, suggesting that the Ni species exist with positive oxidation states.[41,42] The absorption edges of XANES curves have been fitted, and the average oxidation state of Ni species in CdS@Ni is confirmed as 0.89 (Figure S7). Overall, the XAFS investigation clearly verifies that Ni species are atomically dispersed over the surface of the CdS nanowire via Ni–S coordination.

The successful decoration of Ni species over the surface of the CdS nanowire has also been verified by X-ray photoelectron spectroscopy (XPS) analysis (Figure 3A). The high-resolution Ni 2p spectrum in CdS@Ni with peaks at 879.3, 872.2, 863.4, and 854.8 eV are assigned to Ni $2p_{1/2}$, Ni $2p_{3/2}$ and their corresponding satellite peaks, which may suggest the generation of direct Ni–S coordination and exclude Ni–Ni bonding (Figure 3B).[43–45] The dominant S 2p peaks located at 161.3 and 162.5 eV are attributed to lattice sulfur in CdS, while the minor peaks at 160.1 and 161.2 eV correspond to Ni–S bonds (Figure 3C).[46,47] The binding energies of Cd $3d_{5/2}$ and Cd $3d_{3/2}$ are observed at 404.1 and 411.6 eV, revealing a normal Cd^{2+} state, which is ascribed to the Cd–S bonding existing in Ni–CdS (Figure 3D).[48] In addition, compared with those of bare CdS, obvious shifts to a lower binding energy have been observed in both the Cd 3d and S 2p spectra, suggesting that the atomically dispersed Ni causes the increased electron density of the CdS support.[49]

3 | PHOTOCATALYTIC HYDROGEN EVOLUTION

After clarifying the atomic-scale structure of CdS@Ni, we further shifted our attention to the role of isolated Ni atoms in photocatalytic hydrogen evolution. Visible light ($\lambda \geq 400$ nm)-driven photocatalytic H_2 evolution is evaluated while lactic acid is applied as the sacrificial electron donor. The catalytic performance is also influenced by the volume ratio of lactic acid in the reaction system. The optimized performance can be obtained for CdS@Ni

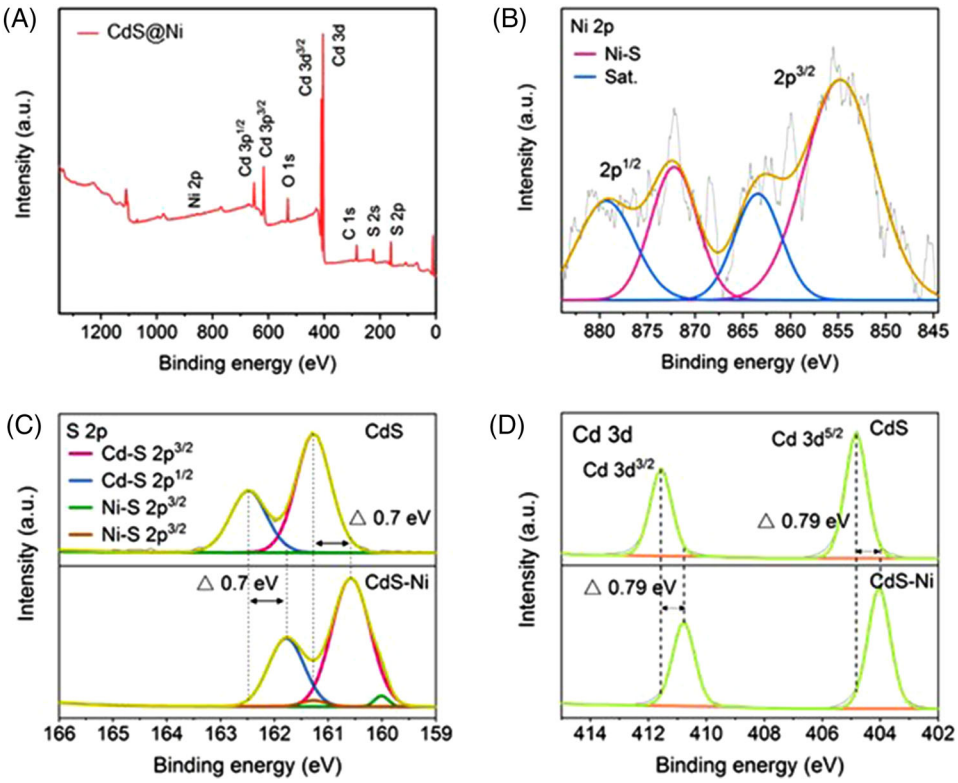

FIGURE 3 (A) Full X-ray photoelectron spectroscopy (XPS) spectrum of CdS@Ni. (B) Ni 2p spectrum of CdS@Ni. (C and D) Comparison of S 2p (C) and Cd 3d (D) spectra between CdS and CdS@Ni. The obvious band shift clearly demonstrates the energy transfer between Ni and CdS

when the volume ratio of lactic acid is 20% (Figure S8). Compared with the pure CdS nanowires, the decoration of Ni species tremendously boosted the catalytic performance. With the increase in the loading contents of Ni species, the H_2 evolution rates also increased accordingly (Figure 4A). Interestingly, the sample with a Ni loading content of 1.35% reached its maximum hydrogen evolution rate of 2.26 mmol g^{-1} h^{-1}/0.452 mmol h^{-1}, which is about 25 times higher than that of the bare CdS nanowires (0.09 mmol g^{-1} h^{-1}). This value is quite impressive and even comparable to those of precious metal-based single-atom photocatalysts (Table S2).[25,50] We may thus be reasonable to conclude that the isolated Ni site performs as the real reactive centers in the hydrogen evolution process.[32] Further increasing the loading content of Ni species has little influence on its catalytic performance, suggesting that the latter Ni sites are not involved in the rate-determining step above a certain surface concentration on CdS. Based on these facts, the optimal CdS@Ni with a Ni loading of 1.35 wt% is chosen for further photocatalytic studies. Control experiments were also conducted to clarify the nature of the hydrogen evolution process under photoirradiation (Figure S9). No H_2 can be detected in the absence of a sacrificial agent in the reaction system, confirming that lactic acid is indispensable in the hydrogen evolution process. The whole reaction was also immediately terminated without light irradiation. These results reveal that hydrogen evolution is indeed driven by photoirradiation.

The stability of the catalyst was further investigated via recycle testing and structural characterization after catalysis (Figure 4B). No obvious degradation of the catalytic performance is observed after five runs. XRD characterization of the sample after catalysis was conducted, and no change was monitored after the reaction, suggesting the high stability of CdS@Ni (Figure S10). The EXAFS and XANES spectra for the sample CdS@Ni after catalysis were also explored, and no obvious change was observed, suggesting that there is no Ni aggregation in the catalytic process and that the coordination configuration of isolated Ni atoms is well maintained after the reaction (Figure S11). The H_2 generation rates of CdS@Ni at different light wavelengths were also explored, in which the catalytic performance qualitatively tracks the visible light absorption spectra (Figure 4C). This result further demonstrates that hydrogen evolution is driven by photoexcitation, while the isolated Ni sites should be the active center for the outstanding photocatalytic activities of CdS@Ni.

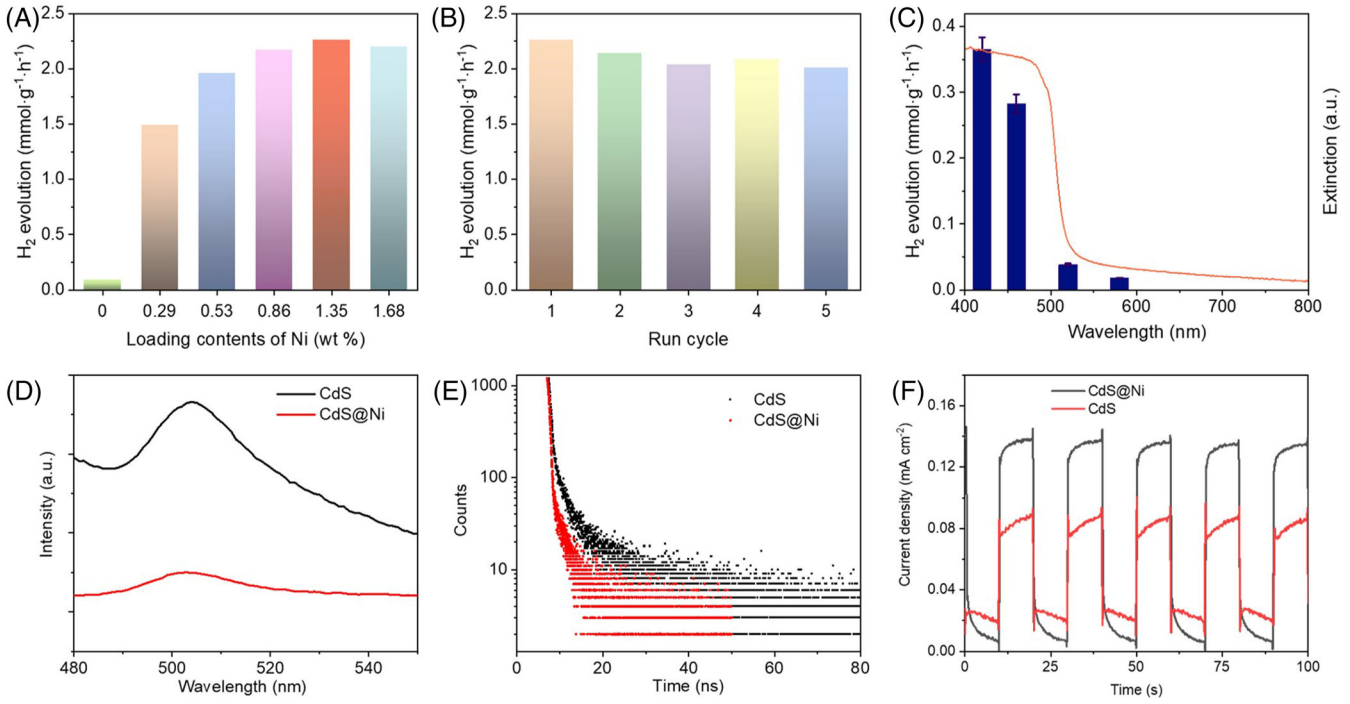

FIGURE 4 (A) H_2 evolution over photocatalysts with different loading contents. (B) Cycling test for H_2 evolution over CdS@Ni. (C) Wavelength-dependent H_2 evolution rates and light absorption spectrum of CdS@Ni. (D) Steady-state photoluminescence (PL) spectra. (E) Time-resolved PL spectra. (F) Transient photocurrent responses of CdS@Ni and CdS

4 | MECHANISM EXPLORATION

The photogenerated electron/hole separation and transfer dynamics have also been conducted to clarify the origin of the greatly boosted photocatalytic performance (Figure S12). As observed, the intrinsic carrier recombination is quite obvious, as evidenced by the strong photoluminescence (PL) intensity (Figure 4D). After Ni decoration, the emission intensity of CdS@Ni is significantly damped, suggesting that the isolated Ni sites can improve the charge carrier separation with impressive trapping ability. To further verify this tentative conclusion, the fluorescence decay times for CdS@Ni and CdS were also explored as 1.158 and 8.175 ns, respectively (Table S3). The significantly quenched fluorescence intensity and the reduced exciton lifetime clearly suggest a significantly accelerated migration of photoexcited electrons to the catalytic active Ni centers of CdS@Ni (Figure 4E).[51,52] The energy transfer (ET) processes have also been quantitatively described via the measurement of the ET efficiency (Φ_{ET}) based on the time-resolved fluorescence decay lifetimes (Equation S1). The Φ_{ET} of CdS@Ni (86.7%) was confirmed based on donor lifetimes in the presence and absence of acceptor molecules, indicating that highly efficient electron transfer was realized after the decoration of Ni. Transient photocurrent responses have been investigated to account for the charge-transfer process (Figure 4F). As expected, the photocurrent density of CdS@Ni is much higher than that of CdS, indicating that the Ni decoration exhibits a better capability to capture electrons and suppress the recombination of photoexcited electron–hole. Therefore, the isolated Ni atom could accelerate the surface reaction kinetics in the catalytic process. This viewpoint is further demonstrated by electrochemical impedance spectroscopy (Figure S13). Lower charge-transfer resistance for CdS@Ni has been confirmed by the evidence that a smaller arch is detected.[53–56] Photo-irradiation can further decrease the arc diameter, suggesting that the isolated Ni atoms act as electron collectors to facilitate the separation of photogenerated electron–hole pairs on the CdS@Ni interface. Thus, an adequate supply of electrons is realized by isolated Ni atoms, optimizing the elementary process of photocatalytic hydrogen evolution.

DFT simulations are also performed to understand the mechanism of the greatly enhanced performance of CdS@Ni. The electron rearrangement between the Ni atoms and S atoms from the CdS supports has been observed, as evidenced by the significantly modified differential electron densities (Figures 5A and S14).[57,58] Compared with pure CdS, the Ni decoration also induces electron transfer from Ni atoms to S atoms and the generation of a new band in the vicinity of the Fermi level. These occupied states of Ni are evolved into the electron trap state for CdS and lift the Fermi level to a position close to the

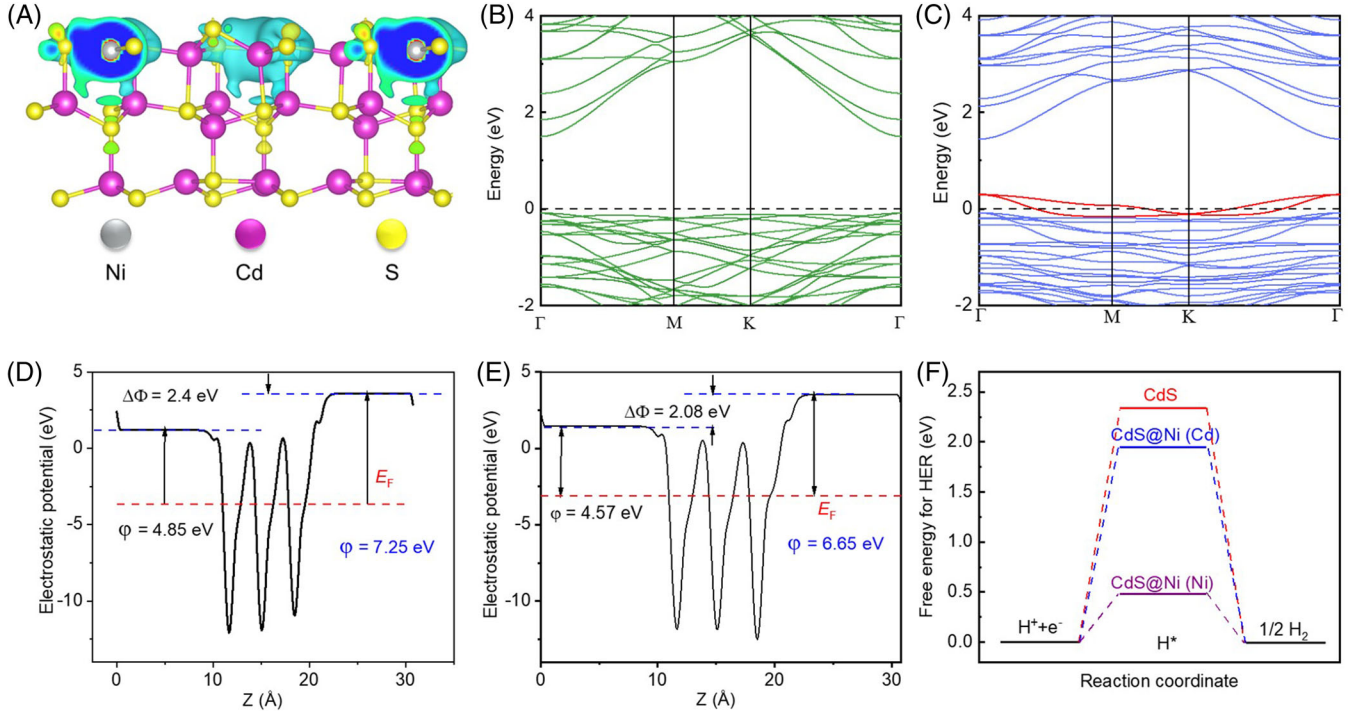

FIGURE 5 (A) Calculated differential charge density for CdS@Ni. (B and C) Band structures of CdS (B) and Ni-decorated CdS (C). (D and E) Calculated work function of CdS (D) and CdS@Ni (E). (F) Gibbs free energy of H* for CdS and CdS@Ni (Cd site and Ni site)

conduction band minimum of CdS, indicating that Ni decoration can act as a mediator to promote electron transfer from CdS to isolated reactive centers (Figure 5B,C).[59–61] Strong electronic coupling between the support and isolated Ni species is thus observed, which also reveals that Ni decoration can boost electron transfer with a narrower bandgap.

The variation in the electrostatic potential of CdS has also been explored (Figure 5D). As documented, the difference between the vacuum level and the Fermi level should numerically equal the work function (Φ). Thus, the work function of the pure CdS (111) facet is confirmed as 2.4 eV.[62] The variation in the electrostatic potential of CdS@Ni has also been investigated, while its work function has been verified as 2.08 eV (Figure 5E). All these results undoubtedly reveal that the work function of CdS@Ni is slightly reduced after Ni decoration, resulting in highly promoted photogenerated electron transfer from CdS to isolated Ni sites.[63] The Gibbs free energy of hydrogen adsorption (ΔG_{H^*}) has also been explored in current research (Figure 5F). The calculated ΔG_{H^*} for pure CdS is confirmed as 2.34 eV, suggesting that hydrogen is not favorably bound to the pure CdS surface. The hydrogen adsorptions are more favorably supported after Ni decoration, as evidenced by the greatly reduced ΔG_{H^*} (0.47 eV) over the Ni sites, which is essential for high catalytic performance.[64,65]

5 | CONCLUSION

In summary, isolated Ni atoms are decorated onto the surface of CdS nanowires via the newly generated Ni–S bonding. Experimental investigation and theoretical studies confirm that strongly stabilized Ni single atoms trigger a continuous and reversible photocatalytic hydrogen evolution process. The photocatalytic hydrogen evolution activity of the optimal CdS@Ni is about 25 times higher than that of the bare CdS nanowires, affording direct evidence that the isolated Ni atoms perform as the real active sites for hydrogen evolution. DFT simulation demonstrates that new electronic states are generated after Ni decoration, which is beneficial for hydrogen adsorption in the hydrogen evolution process, resulting in significantly enhanced catalytic hydrogen evolution capability. Current research will be attractive for the development of earth-abundant reactive centers and inspire the exploration of other semiconductor-based catalysts for photocatalytic energy conversion.

6 | CHARACTERIZATION PROCEDURE

XRD patterns were characterized by X-ray diffractometer with graphite monochromatized Cu-Kα radiation (Bruker, D2 Phaser). UV–vis absorption was characterized by

UV–vis spectroscopy (Shimadzu, UV-2450). PL spectra and fluorescence decay curves were measured using a fluorescent spectrophotometer (Edinburgh, FLSλ80). Fluorescence decay curves were measured using a fluorescent spectrophotometer (Edinburgh, FLSλ80). TEM of the samples was performed with a Titan Themis-Z microscope from Thermo Fisher Scientific by operating it at an accelerating voltage of 300 kV and with a beam current of 0.1–0.4 nA. Dark field imaging was performed by STEM coupled to a high-angle annular dark-field (HAADF) detector. The STEM–HAADF data were acquired with a convergence angle of 20.9 mrad and a HAADF inner angle of 49 mrad. Furthermore, an X-ray energy dispersive spectrometer (FEI SuperX, ≈0.7 sR collection angle, 10 eV dispersion) was also utilized in conjunction with DF-STEM imaging to acquire STEM–EDS spectrum-imaging datasets (image size: 512 × 512 pixels, dwell time 6 μs). Surface chemical analysis was performed by XPS (ULVAC-PHI Inc., PHI Quantera SXM). The molecular weight of the cluster was identified by ESI-MS (Thermo Scientific, Exactive Plus). The Ni contents were detected by ICP–OES (Thermo IRIS Intrepid II XSP spectrometer) after dissolving the samples in a mixture of HCl and HNO_3 (3/1 in volume ratio).

ACKNOWLEDGMENTS

This work received financial support from the King Abdullah University of Science and Technology (KAUST), National Natural Science Foundation of China (22001156), and the Youth Talent Promotion Project of the Science and Technology Association of the Universities of Shaanxi Province (20210602).

CONFLICT OF INTEREST

The authors declare no conflicts of interest.

ORCID

Huabin Zhang https://orcid.org/0000-0003-1601-2471

REFERENCES

1. Xue Z-H, Luan D, Zhang H, Lou XWD. Single-atom catalysts for photocatalytic energy conversion. *Joule*. 2022;6(1):92-133.
2. Shen L, Ma M, Tu F, et al. Recent advances in high-loading catalysts for low-temperature fuel cells: from nanoparticle to single atom. *SusMat*. 2021;1(4):569-592.
3. Lin H, Luo S, Zhang H, Ye J. Toward solar-driven carbon recycling. *Joule*. 2022;6(2):294-314.
4. Li X, Bi W, Zhang L, et al. Single-atom Pt as co-catalyst for enhanced photocatalytic H_2 evolution. *Adv Mater*. 2016;28(12):2427-2431.
5. Zhou Z, Kong Y, Tan H, et al. Cation-vacancy-enriched nickel phosphide for efficient electrosynthesis of hydrogen peroxides. *Adv Mater*. 2022;34(16):e2106541.
6. Zhao S, Yang Y, Tang Z. Insight into structural evolution, active sites, and stability of heterogeneous electrocatalysts. *Angew Chem*. 2022;134(11):e202110186.
7. Yang Y, Yang Y, Liu Y, Zhao S, Tang Z. Metal–organic frameworks for electrocatalysis: beyond their derivatives. *Small Sci*. 2021;1(12):2100015.
8. Zhang H, Zhang P, Qiu M, Dong J, Zhang Y, Lou XW. Ultrasmall MoO_x clusters as a novel cocatalyst for photocatalytic hydrogen evolution. *Adv Mater*. 2019;31(6):1804883.
9. Zhang G, Lan ZA, Wang X. Conjugated polymers: catalysts for photocatalytic hydrogen evolution. *Angew Chem Int Ed*. 2016;55(51):15712-15727.
10. Chen X, Shen S, Guo L, Mao SS. Semiconductor-based photocatalytic hydrogen generation. *Chem Rev*. 2010;110(11):6503-6570.
11. Liao G, Gong Y, Zhang L, Gao H, Yang G-J, Fang B. Semiconductor polymeric graphitic carbon nitride photocatalysts: the "holy grail" for the photocatalytic hydrogen evolution reaction under visible light. *Energy Environ Sci*. 2019;12(7):2080-2147.
12. Tian N, Hu C, Wang J, Zhang Y, Ma T, Huang H. Layered bismuth-based photocatalysts. *Coord Chem Rev*. 2022;463:214515.
13. Xu G, Zhang H, Wei J, et al. Integrating the g-C3N4 Nanosheet with B–H bonding decorated metal–organic framework for CO_2 activation and photoreduction. *ACS Nano*. 2018;12(6):5333-5340.
14. Feng C, Wu Z, Huang KW, Ye J, Zhang H. Surface modification of two-dimensional photocatalysts for solar energy conversion. *Adv Mater*. 2022;34(23):2200180.
15. Wu X, Zuo S, Qiu M, et al. Atomically defined Co on two-dimensional TiO_2 nanosheet for photocatalytic hydrogen evolution. *Chem Eng J*. 2021;420(2):127681.
16. Ran J, Zhang J, Yu J, Jaroniec M, Qiao SZ. Earth-abundant cocatalysts for semiconductor-based photocatalytic water splitting. *Chem Soc Rev*. 2014;43(22):7787-7812.
17. Yang J, Wang D, Han H, Li C. Roles of cocatalysts in photocatalysis and photoelectrocatalysis. *Acc Chem Res*. 2013;46(8):1900-1909.
18. Fu Y, Liao Y, Li P, et al. Layer structured materials for ambient nitrogen fixation. *Coord Chem Rev*. 2022;460:214468.
19. Wu X, Zhang H, Zuo S, et al. Engineering the coordination sphere of isolated active sites to explore the intrinsic activity in single-atom catalysts. *Nano-Micro Lett*. 2021;13(1):1-28.
20. Zhang H, Cheng W, Luan D, Lou XW. Atomically dispersed reactive centers for electrocatalytic CO_2 reduction and water splitting. *Angew Chem Int Ed*. 2021;60(24):13177-13196.
21. Zhang H, Zuo S, Qiu M, et al. Direct probing of atomically dispersed Ru species over multi-edged TiO_2 for highly efficient photocatalytic hydrogen evolution. *Sci Adv*. 2020;6(39):eabb9823.
22. Qureshi M, Garcia-Esparza AT, Jeantelot G, et al. Catalytic consequences of ultrafine Pt clusters supported on $SrTiO_3$ for photocatalytic overall water splitting. *J Catal*. 2019;376:180-190.
23. Jeantelot G, Qureshi M, Harb M, et al. TiO_2-supported Pt single atoms by surface organometallic chemistry for photocatalytic hydrogen evolution. *Phys Chem Chem Phys*. 2019;21(44):24429-24440.
24. Gao C, Low J, Long R, Kong T, Zhu J, Xiong Y. Heterogeneous single-atom photocatalysts: fundamentals and applications. *Chem Rev*. 2020;120(21):12175-12216.
25. Xia B, Zhang Y, Ran J, Jaroniec M, Qiao S-Z. Single-atom photocatalysts for emerging reactions. *ACS Cent Sci*. 2021;7(1):39-54.

26. Lee B-H, Park S, Kim M, et al. Reversible and cooperative photoactivation of single-atom Cu/TiO_2 photocatalysts. *Nat Mater*. 2019;18(6):620-626.
27. Liu W, Wang P, Ao Y, et al. Directing charge transfer in chemical-bonded $BaTiO_3$@ReS_2 Schottky heterojunction for piezoelectric enhanced photocatalysis. *Adv Mater*. 2022. https://doi.org/10.1002/adma.202202508
28. Zhou P, Chen H, Chao Y, et al. Single-atom Pt-I_3 sites on all-inorganic Cs2SnI6 perovskite for efficient photocatalytic hydrogen production. *Nat Commun*. 2021;12(1):1-8.
29. Jiang XH, Zhang LS, Liu HY, et al. Silver single atom in carbon nitride catalyst for highly efficient photocatalytic hydrogen evolution. *Angew Chem*. 2020;132(51):23312-23316.
30. Zhou X, Hwang I, Tomanec O, et al. Advanced photocatalysts: pinning single atom co-catalysts on titania nanotubes. *Adv Funct Mater*. 2021;31(30):2102843.
31. Ge L, Zuo F, Liu J, et al. Synthesis and efficient visible light photocatalytic hydrogen evolution of polymeric g-C3N4 coupled with CdS quantum dots. *J Phys Chem*. 2012;116(25):13708-13714.
32. Li W, Chu X-S, Wang F, et al. Pd single-atom decorated CdS nanocatalyst for highly efficient overall water splitting under simulated solar light. *Appl Catal B*. 2022;304:121000.
33. Thang HV, Pacchioni G, DeRita L, Christopher P. Nature of stable single atom Pt catalysts dispersed on anatase TiO_2. *J Catal*. 2018;367:104-114.
34. Wan J, Chen W, Jia C, et al. Defect effects on TiO_2 nanosheets: stabilizing single atomic site Au and promoting catalytic properties. *Adv Mater*. 2018;30(11):1705369.
35. Wang G, He C-T, Huang R, Mao J, Wang D, Li Y. Photoinduction of Cu single atoms decorated on UiO-66-NH_2 for enhanced photocatalytic reduction of CO_2 to liquid fuels. *J Am Chem Soc*. 2020;142(45):19339-19345.
36. Ji S, Qu Y, Wang T, et al. Rare-earth single erbium atoms for enhanced photocatalytic CO_2 reduction. *Angew Chem Int Ed*. 2020;59(26):10651-10657.
37. Zeiri L, Patla I, Acharya S, Golan Y, Efrima S. Raman spectroscopy of ultranarrow CdS nanostructures. *J Phys Chem*. 2007;111(32):11843-11848.
38. Liang S, Liu S, Guo M, Zhang M. Highly dispersed potassium-based nanowire structure for selectively capturing trace hydrogen chloride in H_2S/CO_2 environments. *Energy Fuels*. 2020;34(9):11712-11716.
39. Zhang H, Wang Y, Zuo S, Zhou W, Zhang J, Lou XWD. Isolated cobalt centers on $W_{18}O_{49}$ nanowires perform as a reaction switch for efficient CO_2 photoreduction. *J Am Chem Soc*. 2021;143(5):2173-2177.
40. Zhang H, Wei J, Dong J, et al. Efficient visible-light-driven carbon dioxide reduction by a single-atom implanted metal–organic framework. *Angew Chem*. 2016;128(46):14522-14526.
41. Zhang H, Yu L, Chen T, Zhou W, Lou XW. Surface modulation of hierarchical MoS_2 nanosheets by Ni single atoms for enhanced electrocatalytic hydrogen evolution. *Adv Funct Mater*. 2018;28(51):1807086.
42. Zhang H, Zhou W, Chen T, et al. A modular strategy for decorating isolated cobalt atoms into multichannel carbon matrix for electrocatalytic oxygen reduction. *Energy Environ Sci*. 2018;11(8):1980-1984.
43. Nesbitt H, Legrand D, Bancroft G. Interpretation of Ni_2P XPS spectra of Ni conductors and Ni insulators. *Phys Chem Miner*. 2000;27(5):357-366.
44. Vu M-H, Sakar M, Nguyen C-C, Do T-O. Chemically bonded Ni cocatalyst onto the S doped g-C_3N_4 nanosheets and their synergistic enhancement in H_2 production under sunlight irradiation. *ACS Sustain Chem Eng*. 2018;6(3):4194-4203.
45. Wu Y, He H. Direct-current electrodeposition of Ni–S–Fe alloy for hydrogen evolution reaction in alkaline solution. *Int J Hydrog Energy*. 2018;43(4):1989-1997.
46. Hota G, Idage S, Khilar KC. Characterization of nano-sized CdS–Ag_2S core–shell nanoparticles using XPS technique. *Colloids Surf A: Physicochem Eng Asp*. 2007;293(1-3):5-12.
47. Abe T, Kashiwaba Y, Baba M, Imai J, Sasaki H. XPS analysis of p-type Cu-doped CdS thin films. *Appl Surf Sci*. 2001;175:549-554.
48. Tao J, Liu J, Chen L, et al. 7.1% efficient co-electroplated Cu_2ZnSnS_4 thin film solar cells with sputtered CdS buffer layers. *Green Chem*. 2016;18(2):550-557.
49. Liu G, Li P, Zhao G, et al. Promoting active species generation by plasmon-induced hot-electron excitation for efficient electrocatalytic oxygen evolution. *J Am Chem Soc*. 2016;138(29):9128-9136.
50. Zhang F, Zhu Y, Lin Q, Zhang L, Zhang X, Wang H. Noble-metal single-atoms in thermocatalysis, electrocatalysis, and photocatalysis. *Energy Environ Sci*. 2021;14(5):2954-3009.
51. Xiang X, Zhu B, Cheng B, Yu J, Lv H. Enhanced photocatalytic H_2-production activity of CdS quantum dots using Sn^{2+} as cocatalyst under visible light irradiation. *Small*. 2020;16(26):2001024.
52. Yu H, Liu R, Wang X, Wang P, Yu J. Enhanced visible-light photocatalytic activity of Bi_2WO_6 nanoparticles by Ag_2O cocatalyst. *Appl Catal B*. 2012;111-112:326-333.
53. Zuo S, Wu ZP, Zhang H, Lou XW. Operando monitoring and deciphering the structural evolution in oxygen evolution electrocatalysis. *Adv Energy Mater*. 2022;12(8):2103383.
54. Wu ZP, Zhang H, Zuo S, et al. Manipulating the local coordination and electronic structures for efficient electrocatalytic oxygen evolution. *Adv Mater*. 2021;33(40):2103004.
55. Li Y, Zuo S, Li Q-H, et al. Vertically aligned MoS_2 with in-plane selectively cleaved Mo–S bond for hydrogen production. *Nano Lett*. 2021;21(4):1848-1855.
56. Huang W-H, Li X-M, Yang X-F, Zhang H-B, Wang F, Zhang J. Highly efficient electrocatalysts for overall water splitting: mesoporous CoS/MoS_2 with hetero-interfaces. *ChemComm*. 2021;57(39):4847-4850.
57. Zhang H, Ma Z, Duan J, et al. Active sites implanted carbon cages in core–shell architecture: highly active and durable electrocatalyst for hydrogen evolution reaction. *ACS Nano*. 2016;10(1):684-694.
58. Deng J, Ren P, Deng D, Bao X. Enhanced electron penetration through an ultrathin graphene layer for highly efficient catalysis of the hydrogen evolution reaction. *Angew Chem Int Ed*. 2015;54(7):2100-2104.
59. Zhang Y, Zhou W, Tang Y, et al. Unravelling unsaturated edge S in amorphous NiS_x for boosting photocatalytic H2 evolution of metastable phase CdS confined inside hydrophilic beads. *Appl Catal B*. 2022;305:121055.
60. Hafner J. Ab initio simulations of materials using VASP: density-functional theory and beyond. *J Comput Chem*. 2008;29(13):2044-2078.

61. Zhu J, Jin H, Chen W, et al. Structural and electronic properties of a W_3O_9 cluster supported on the TiO_2 (110) surface. *J Phys Chem*. 2009;113(40):17509-17517.
62. Kahn A. Fermi level, work function and vacuum level. *Mater Horiz*. 2016;3(1):7-10.
63. Shi J, Islam IU, Chen W, et al. Two-dimensional ultrathin $Zn_xCd_{1-x}S$ nanosheet with exposed polar facet by using layered double hydroxide template for photocatalytic hydrogen generation. *Int J Hydrog Energy*. 2018;43(42):19481-19491.
64. Zhang H, An P, Zhou W, et al. Dynamic traction of lattice-confined platinum atoms into mesoporous carbon matrix for hydrogen evolution reaction. *Sci Adv*. 2018;4(1):eaao6657.
65. Qu Y, Pan H, Kwok CT, Wang Z. A first-principles study on the hydrogen evolution reaction of VS_2 nanoribbons. *Phys Chem Phys*. 2015;17(38):24820-24825.

AUTHOR BIOGRAPHIES

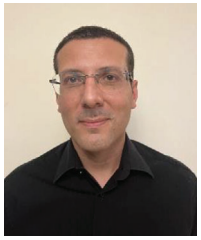

Samy Ould-Chikh obtained his Ph.D. degree in chemistry in 2008 from the Ecole Normale superieure in Lyon under the mentorship of Prof. M. Hemati. After pursuing research interests in photocatalysis science at IRCE-Lyon (Lyon, France), he moved to King Abdullah University of Science and Technology (Thuwal, Saudi Arabia) as a postdoctoral fellow. He was appointed research scientist in 2012 to handle the operando characterization of catalysts using multiple imaging and spectroscopic techniques.

Wei Zhou is an Associated Professor in Department of Applied Physics, School of Science, Tianjin University, China. He received his PhD degree in Materials Physics and Chemistry from Tianjin University in 2010, and worked as a Visiting Scholar for three years in WPI-MANA of NIMS, Japan. His recent interest has focused on theoretically and experimentally designing advanced 2D materials for photocatalytic, electrocatalytic and spintronics applications. Until now, he has published over 100 in-peer reviewed papers.

Huabin Zhang received his Ph.D. degree in chemistry from the Fujian Institute of Research on the Structure of Matter, Chinese Academy of Sciences (FJIRSM-CAS). After finishing his postdoc research in Japan at the National Institute of Materials Science (NIMS) and Singapore at Nanyang Technological University, Singapore, he joined KAUST serving as an Assistant Professor in January 2021. His research interests focus on advanced catalysis for sustainable energy.

SUPPORTING INFORMATION

Additional supporting information can be found online in the Supporting Information section at the end of this article.

How to cite this article: Huang W, Bo T, Zuo S, et al. Surface decorated Ni sites for superior photocatalytic hydrogen production. *SusMat*. 2022;2:466–475. https://doi.org/10.1002/sus2.76